Numerical simulation of a Penning trap

Alessio Canclini, Filip von der Lippe
(Dated: October 25, 2022)

We implement a numerical simulation of a Penning trap by solving a system of coupled differential equations. Analysis shows the superiority of the fourth order Runge-Kutta (RK4) method over the forward Euler method. We have a convergence rate of 1.397 for Euler compared to 4 for RK4. The RK4s high precision allows accurate simulations for a relatively low value of $N = 5000$. Running the simulation with and without Coulomb interaction between particles gives different results indicating that interaction plays an important role in particle motion within the trap. Finally, exploring resonance phenomena, we find three frequency domains resulting in all particles escaping, or rather, being ejected from the trap after a period of 500 μs. For the remaining frequencies close to no particles escape. A more fine-grained frequency scan is performed for one of the resonance domains showing that particle interaction again is an important factor.

I. INTRODUCTION

The purpose of this report is to present the study of the effects of a Penning trap through numerical simulations. The Penning trap is a device used to store or "trap" charged particles using static electric and magnetic fields as shown in figure 1. These particles can then be used for a variety of experiments. Examples of this are the ALPHA, AEgIS and BASE experiments at CERN, these use Penning traps to control antimatter. The electric field is generated by two end caps (a), at the top and bottom, and a ring (b) (figure 1 only shows the ring cross-section). This electric field restricts the particles' movement in the z direction and the additional homogenous magnetic field hinders particles escaping in the xy-plane (radial direction) if it is strong enough. The magnetic field is set by a cylinder magnet (c) (figure 1 again only shows the ring cross-section).

Materials to construct a physical Penning trap are very costly, we will therefore be using a numerical approach to simulate a Penning trap. To implement such a simulation we will be working with a system of coupled non-linear differential equations. These are very difficult and often impossible to solve analytically. In addition to the material cost, the complexity of the equations therefore also motivates the use of numerical methods.

We will first explore the basic behavior of the Penning trap simulation and then look into some Penning trap physics. Expecting the trap to be a system with complicated periodic particle motions, we will subject the trap to a time-dependent electromagnetic field to look for possible resonance phenomena.

Section II will describe the mathematical and physical background as well as concrete algorithms which in this case will be implemented in C++, but can be written in any programming language.

In section III we present a selection of results form different simulations and an error analysis. This will include simulations with a single particle, 2 particles and 100 random particles.

A detailed discussion of the algorithms' and results is presented in section IV, followed by a summary and potential for further experiments in section V.

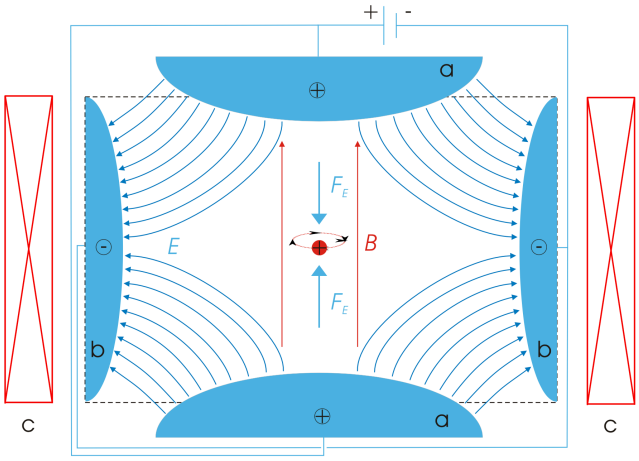

FIG. 1. This figure shows the idea of a Penning trap with a red positively charged particle in the center. Here blue lines represent the electric field generated by a quadrupole consisting of end caps (a) and a ring electrode (b). The red lines represent the magnetic field created by a surrounding cylinder magnet (c). Illustration by Arian Kriesch taken from Wikimedia Commons.

II. METHODS

The physical laws used to implement the Penning trap simulation will be from electrodynamics and classical mechanics, we will not take quantum aspects into account. The following equations will be used:

$$\mathbf{E} = -\nabla V \tag{1}$$

$\mathbf{E}$ is the electric field and V the electric potential.

$$\mathbf{E}(\mathbf{r}) = k_e \sum_{j=1}^{n} q_j \frac{\mathbf{r} - \mathbf{r}_j}{|\mathbf{r} - \mathbf{r}_j|^3} \tag{2}$$

$\mathbf{E}(\mathbf{r})$ is the electric field at a point $\mathbf{r}$. This is set up by point charges $q_1, ..., q_n$ at points $\mathbf{r}_1, ..., \mathbf{r}_n$. This comes

from **Coulomb's law**, stating the magnitude of force between to point charges. $k_e \approx 8.988 \cdot 10^9 Nm^2C^{-2}$ is the Coulomb constant.

$$\mathbf{F} = q\mathbf{E} + q\mathbf{v} \times \mathbf{B} \tag{3}$$

This is the **Lonretz force**, the force $\mathbf{F}$ on a particle with charge q, an electric field $\mathbf{E}$, magnetic field $\mathbf{B}$ and velocity of the particle $\mathbf{v}$.

$$m\ddot{\mathbf{r}} = \sum_i \mathbf{F}_i \tag{4}$$

Eq. 4 is Newton's second law. Here m is the mass of the particle and $\ddot{\mathbf{r}} \equiv \frac{d^2\mathbf{r}}{dt^2}$ the acceleration. Famously expressing that the sum of external forces equals mass times acceleration.

$$V(x, y, z) = \frac{V_0}{2d^2}(2z^2 - x^2 - y^2) \tag{5}$$

For this experiment we will be considering an ideal Penning trap for which the electric field $\mathbf{E}$ is given by the electric potential V. Here V_0 is the potential applied to the electrodes. The trap will be approximated as a sphere where $d = \sqrt{z_0^2 + r_0^2/2}$ is the *charachteristic dimension* representing the length scale (or radius of the sphere) for the region between electrodes. Here z_0 is the distance from the center to the end caps (a) and r_0 is the distance from the center to the surrounding ring (b).

$$\mathbf{B} = B_0\hat{e}_z = (0, 0, B_0) \tag{6}$$

$\mathbf{B}$ is the homogenous magnetic field and is dictated by the field strength B_0. With $B_0 > 0$.

Equations for single particle motion

Now starting from Newton's second law and using the equations above we can express the time evolution of a single particle's motion. The sum of forces will be the Lonretz force. Putting eq. 3 into eq. 4 leads to:

$$m\ddot{\mathbf{r}} = q\mathbf{E} + q\mathbf{v} \times \mathbf{B} \tag{7}$$

Here $\ddot{\mathbf{r}} = (\ddot{x}, \ddot{y}, \ddot{z})$ and $\mathbf{v} = (\dot{x}, \dot{y}, \dot{z})$. Putting eq. 5 into eq. 1 gives us:

$$\mathbf{E} = \left(x\frac{v_0}{d^2}, y\frac{v_0}{d^2}, -2z\frac{v_0}{d^2}\right) \tag{8}$$

Now looking at $q\mathbf{v} \times \mathbf{B}$ we have:

$$(q\dot{x}, q\dot{y}, q\dot{z}) \times (0, 0, B_0) = (B_0q\dot{y}, -B_0q\dot{x}, 0) \tag{9}$$

Finally substituting for $\mathbf{E}$ and $q\mathbf{v} \times \mathbf{B}$ in eq. 7 results in:

$$m\begin{pmatrix}\ddot{x}\\ \ddot{y}\\ \ddot{z}\end{pmatrix} = \begin{pmatrix}qx\frac{v_0}{d^2}\\ qy\frac{v_0}{d^2}\\ -2qz\frac{v_0}{d^2}\end{pmatrix} + \begin{pmatrix}B_0q\dot{y}\\ -B_0q\dot{x}\\ 0\end{pmatrix}$$

Rewriting this as a set of equations leaves us with:

$$\ddot{x} - w_0\dot{y} - \frac{1}{2}w_z^2x = 0 \tag{10}$$

$$\ddot{y} + w_0\dot{x} - \frac{1}{2}w_z^2y = 0 \tag{11}$$

$$\ddot{z} + w_z^2z = 0 \tag{12}$$

Where $w_0 = \frac{qB_0}{m}$ and $w_z^2 = \frac{2qV_0}{md^2}$. Taking a closer look at eq. 12 we see that the general solution is:

$$z = A\cos(w_zt) + B\sin(w_zt) \tag{13}$$

eq. 10 and 11 are coupled, thus introducing a challenge. This can be resolved by introducing a complex function $f(t) = x(t) + iy(t)$ and rewriting them as a single differential equation. By introducing the complex function we have:

$$f(t) = x(t) + iy(t) \tag{14}$$

$$\dot{f}(t) = \dot{x}(t) + i\dot{y}(t) \tag{15}$$

$$\ddot{f}(t) = \ddot{x}(t) + i\ddot{y}(t) \tag{16}$$

Now multiplying eq. 11 by i gives:

$$i\ddot{y} + iw_0\dot{x} - i\frac{1}{2}w_z^2y = 0 \tag{17}$$

eq. 10 and 17 can then be summed:

$$\ddot{x} + i\ddot{y} - w_0\dot{y} + iw_0\dot{x} - \frac{1}{2}w_z^2x - i\frac{1}{2}w_z^2y = 0 \tag{18}$$

Finally, substituting for $f(t)$, $\dot{f}(t)$ and $\ddot{f}(t)$ shows that eq. 10 and 11 can be rewritten as a single differential equation for f:

$$\ddot{f} + iw_0\dot{f} - \frac{1}{2}w_z^2f = 0 \tag{19}$$

The general solution to eq. 19 is:

$$f(t) = A_+e^{-i(w_+t+\phi_+)} + A_-e^{-i(w_-t+\phi_-)} \tag{20}$$

where the amplitudes A_+ and A_- are positive, ϕ_+ and ϕ_- are constant phases, and

$$w_\pm = \frac{w_0 \pm \sqrt{w_0^2 - 2w_z^2}}{2} \tag{21}$$

To obtain a bounded solution for the radial movement (xy-plane) of the particle we need to introduce some constraints on w_0 and w_z. In other words we will introduce some constraints that will ensure that $|f(t)| < \infty$ as $t \to \infty$.

Studying eq. 20 one notices that $|f(t)| \to \infty$ only if $w_\pm$ is complex. To avoid this, we introduce the limitation $w_0^2 - 2w_z^2 \geq 0$, avoiding any negative values inside the square root and consequently limiting the result to real numbers. Rearranging this and remembering that $w_0 = \frac{qB_0}{m}$ and $w_z^2 = \frac{2qV_0}{md^2}$ leaves us with:

$$\frac{q}{m} \geq \frac{4V_0}{B_0^2d^2} \tag{22}$$

A constraint, that if satisfied, keeps the particle within the Penning trap.

Upper and lower bounds

Now to express the upper and lower bounds of the particles' distance from the origin in the xy-plane we start with eq. 20. Through Taylor expansion of e^{ix} we arrive at Euler's formula:

$$e^{ix} = \cos(x) + i\sin(x)$$

Introducing $u = w_+t + \phi_+$ and $v = w_-t + \phi_-$, and using Euler's formula, eq. 20 can be rewritten as:

$$f(t) = A_+\left(\cos(u) - i\sin(u)\right) + A_-\left(\cos(v) - i\sin(v)\right)$$

The physical coordinates can then be found as $x(t) = \mathrm{Re}\, f(t)$ and $y(t) = \mathrm{Im}\, f(t)$. Giving us:

$$\begin{aligned} x(t) &= A_+\cos(u) + A_-\cos(v) \\ y(t) &= -A_+\sin(u) - A_-\sin(v) \end{aligned}$$

Since our xy-plane is a circle, the particle's distance from the origin can be expressed as the radius $R = \sqrt{x^2 + y^2}$. Substituting for x and y we have:

$$\begin{aligned} R =&[(A_+\cos(u) + A_-\cos(v))^2 \\ &+ (-A_+\sin(u) - A_-\sin(v))^2]^{1/2} \end{aligned}$$

After expanding and rearranging we have:

$$\begin{aligned} R =&[A_+^2(\cos^2(u) + \sin^2(u)) + A_-^2(\cos^2(v) + \sin^2(v)) \\ &+ 2A_+A_-(cos(u)\cos(v) + \sin(u)\sin(v))]^{1/2} \end{aligned}$$

Recognizing that $cos^2(u) + \sin^2(u) = 1$ and $cos(u)\cos(v) + \sin(u)\sin(v) = \cos(u - v)$ this can be simplified to:

$$R = \sqrt{A_+^2 + A_-^2 + 2A_+A_-\cos(u - v)}$$

We know that cos is a function with an upper bound of 1 and lower bound of -1. The bounds for R are consequently:

$$\begin{aligned} R_+ &= \sqrt{A_+^2 + 2A_+A_- + A_-^2} = A_+ + A_- \\ R_- &= \sqrt{A_+^2 - 2A_+A_- + A_-^2} = |A_+ - A_-| \end{aligned}$$

Numbers and units

The following units will be used for all simulation experiments:

- Length: micrometer (μm)
- Time: microseconds (μs)
- Mass: atomic mass unit (u)
- Charge: the elementary charge (e)

With these units we end up with a Coulomb constant equal to:

- $k_e = 1.38935333 \times 10^5 \frac{\mathrm{u}(\mu\mathrm{m})^3}{(\mu\mathrm{s})^2(\mathrm{e})^2}$

SI units for Tesla (magnetic field strength) and Volt (electric potential) become:

- $T = 9.64852558 \times 10^1 \frac{\mathrm{u}}{(\mu\mathrm{s})\mathrm{e}}$
- $V = 9.64852558 \times 10^7 \frac{\mathrm{u}(\mu\mathrm{m})^2}{(\mu\mathrm{s})^2\mathrm{e}}$

With these units the default penning trap configuration will be:

- $B_0 = 1.00\ \mathrm{T} = 9.65 \times 10^1 \frac{\mathrm{u}}{(\mu\mathrm{s})\mathrm{e}}$
- $V_0 = 25.0\ \mathrm{mV} = 2.41 \times 10^6 \frac{\mathrm{u}(\mu\mathrm{m})^2}{(\mu\mathrm{s})^2\mathrm{e}}$
- $d = 500\mu\mathrm{m}$

Particles

Our charged particles will be singly-charged Calcium ions (Ca^+) with a mass of 40.077u.

- Particle 1:
  $(x_0, y_0, z_0) = (20, 0, 20)\mu\mathrm{m}$
  $(v_{x,0}, v_{y,0}, v_{z,0}) = (0, 25, 0)\mu\mathrm{m}/\mu\mathrm{s}$
- Particle 2:
  $(x_0, y_0, z_0) = (25, 25, 0)\mu\mathrm{m}$
  $(v_{x,0}, v_{y,0}, v_{z,0}) = (0, 40, 5)\mu\mathrm{m}/\mu\mathrm{s}$

Simulations with one particle will use initial conditions for Particle 1 whilst simulations with two particles will use both Particle 1 and Particle 2. For further simulations with 100 particles, Armadillo's `vec::randu()` function will be used to generate random initial positions and velocities for each particle.

Specific analytical solution

To test the numerical solutions and for error analysis an analytical solution for Particle 1 is used. For these initial condition the specific $z(t)$ solution for eq. II becomes:

$$z(t) = z_0\cos(\omega_z t)$$

The specific solution for motion in the xy-plane, $f(t)$ is given by eq. 20 with

$$\begin{aligned} A_+ = \frac{v_0 + \omega_- x_0}{\omega_- - \omega_+}, \quad A_- = -\frac{v_0 + \omega_+ - x_0}{\omega_- - \omega_+} \\ \phi_+ = 0, \quad \phi_- = 0 \end{aligned}$$

Equations for multiple particle motion

For all simulations with more than one particle when particle interaction is taken into account, the equations of motion will be coupled because of the Coulomb force between two point charges. Our numerical algorithms will therefore be solving the following second-order differential equations:

$$\ddot{x}_i - w_{0,i}\dot{y}_i - \frac{1}{2}w_{z,i}^2 x_i - k_e \frac{q_i}{m_i}\sum_{j\neq i}^{n} q_j \frac{x_i - x_j}{|\mathbf{r}_i - \mathbf{r}_j|^3} = 0 \quad (23)$$

$$\ddot{y}_i + w_{0,i}\dot{x}_i - \frac{1}{2}w_{z,i}^2 y_i - k_e \frac{q_i}{m_i}\sum_{j\neq i}^{n} q_j \frac{y_i - y_j}{|\mathbf{r}_i - \mathbf{r}_j|^3} = 0 \quad (24)$$

$$\ddot{z}_i + w_{z,i}^2 z_i - k_e \frac{q_i}{m_i}\sum_{j\neq i}^{n} q_j \frac{z_i - z_j}{|\mathbf{r}_i - \mathbf{r}_j|^3} = 0 \quad (25)$$

Here the summation term is the Coulomb force and i and j are particle indices for n particles with charges $\{q_1, ..., q_n\}$ and masses $\{m_1, .., m_n\}$.

To numerically solve the above equations they will be reformulated as coupled first-order differential equations:

$$\dot{\mathbf{r}} = \mathbf{v} \quad (26)$$

$$\dot{\mathbf{v}} = \frac{\mathbf{F}}{m} \quad (27)$$

The algorithms

To evolve our Penning trap system in time the following algorithms will be implemented to solve our particles' equations of motion. Consider the forward difference approximation for the first derivative based on Taylor expansion:

$$y_n' = \frac{y_{n+1} - y_n}{h}, \quad h = t_{t-1} - t_n \quad (28)$$

Rearranging this results in the forward Euler method which has a local error of $\mathcal{O}(h^2)$ and global error of $\mathcal{O}(h)$, making it only first order accurate. The method is easy to implement and will be used for comparisons and checking of the main algorithm.

Algorithm 1 Forward Euler method

procedure FORWARD EULER(y_0, h)
- $y' = f(t_i, y_i)$ ▷ Single fist-order diff. eq.
- $n = 1/h$ ▷ Compute number of steps

for $i = 0, 1, 2, \ldots, n$ **do**
- $y_{i+1} = y_i + hf(t_i, y_i)$ ▷ Value at next time step

Similarly to the forward Euler, Runge-Kutta fourth order (RK4) is based on Taylor expansion, but by adding several intermediate steps to the computation of y_{i+1} it generally yields better solutions for ODEs. RK4 has a local error of $\mathcal{O}(h^5)$ and global error of $\mathcal{O}(h^4)$. (REF COMPENDIUM HERE)

Algorithm 2 Runge-Kutta fourth order method

procedure RUNGE-KUTTA FOURTH ORDER(y_0, h)
- $y' = f(t_i, y_i)$ ▷ Single fist-order diff. eq.
- $n = 1/h$ ▷ Compute number of steps

for $i = 0, 1, 2, \ldots, n$ **do**
- $k_1 = hf(t_i, y_i)$ ▷ Intermediate step 1
- $k_2 = hf(t_i + h/2, y_i + k_1/2)$ ▷ Intermediate step 2
- $k_3 = hf(t_i + h/2, y_i + k_2/2)$ ▷ Intermediate step 3
- $k_4 = hf(t_i + h, y_i + k_3)$ ▷ Intermediate step 4
- $y_{i+1} = y_i + \frac{1}{6}(k_1 + 2k_2 + 2k_3 + k_4)$ ▷ Final algorithm

The RK4 scheme will be our main method as this is a "gold standard" in numerical analysis. Early tests with one single particle will be confirmed by an analytical solution, but for comparison of more complex scenarios the simple forward Euler scheme will also be implemented.

The Penning trap with time evolving algorithms will be implemented in an object-oriented C++ code, the plots are generated using Python.

Resonance experiments

We will be subjecting the Penning trap to a time-dependent electromagnetic field by adding a time-dependent perturbation to the electric potential with a constant amplitude f and angular frequency ω_V. For resonance experiments the following replacement will be made:

$$V_0 \rightarrow V_0(1 + f\cos(\omega_V t)) \quad (29)$$

The simulation is run for 500 μs for amplitudes $f = 0.1, 0.4, 0.7$ and frequencies $\omega_V \in [0.2, 2.5]$ MHz. The frequency range is initially explored with a step size of 0.2 MHz disregarding Coulomb interactions. An area of interest (in this case $\omega_V \in (2.05, 2.35)$) is then looked at closely with smaller step sizes of 0.001 MHz once with Coulomb interactions and once without.

Error analysis

To check the validity of our methods and gauge how realistic our Penning trap simulations are, we perform an error analysis of the numerical methods implemented. This is done by considering the simple case of a single particle, making it easy to compare the numerical to analytic results. The simulation with Particle 1 is run over 50 μs. This is done for four different step

sizes $h_k = 50/n_k \mu$s. The chosen step sizes are for $n_1 = 4000, n_2 = 8000, n_3 = 16000, n_4 = 32000$. For each step size the relative error of $\mathbf{r}_i$ for each time step t_i is calculated for both algorithms. Additionally, these results are used to calculate the error convergence rate in both cases.

III. RESULTS

First we test our Penning trap's behavior for a single particle to see if it produces the expected motion in this simple case. All three solutions have been plotted in figure 2 for $N = 10000$ steps to examine weather the numerical and analytic results agree.

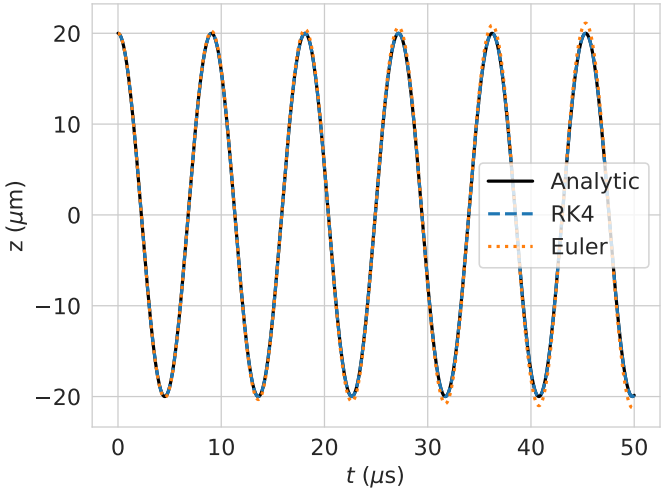

FIG. 2. Here we see the vertical path of a single particle over 50 μs for $N = 10000$. The analytic, Euler and RK4 solutions are shown.

Figure 2 shows that both the forward Euler and RK4 method show the same z motion as the analytic solution for a single particle. The particle oscillates vertically but over time we notice a growing error for the Euler method, While RK4 seems to agree well with the analytic solution.

We again compare the three solutions but now using a smaller time step of $n = 5000$.

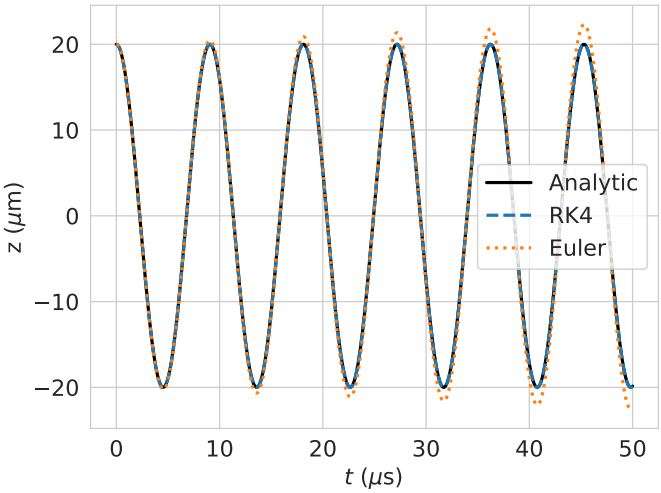

FIG. 3. Here we see the vertical path of a single particle over 50 μs for $N = 5000$. The analytic, Euler and RK4 solutions are shown.

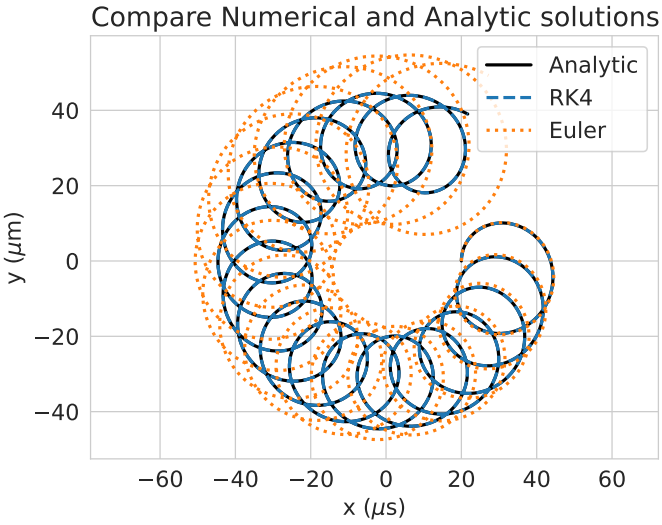

FIG. 4. Horizontal motion of a single particle over 50 μs for $N = 10000$. The analytic, Euler and RK4 solutions are shown.

Figure 4 displays that the numerical methods perform similarly for all spatial axes of the simulation.

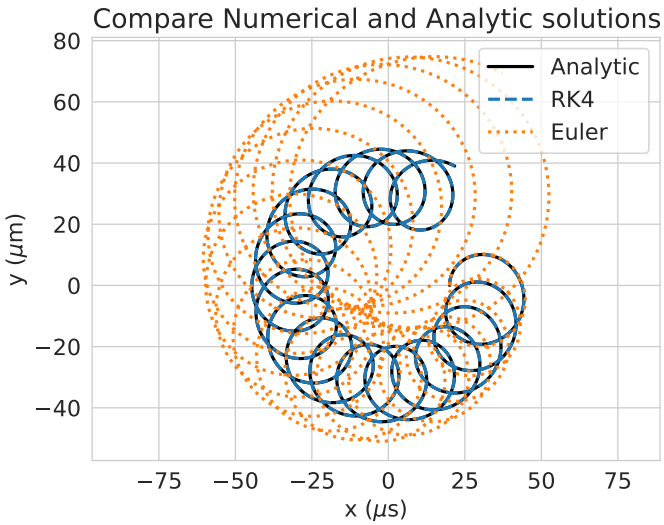

FIG. 5. Horizontal motion of a single particle over 50 μs for $N = 5000$. The analytic, Euler and RK4 solutions are shown.

Above in figure 3 and 5 we see a growing error for Euler while RK4 still agrees well with the analytic solution. We also notice that a change in number of timesteps from $N = 10000$ to $N = 5000$ impacts the performence of the Euler method, while RK4 keeps its accuracy indicating the superiority of this method. All this means that we now especially can trust the RK4 method but also Euler while keeping the timestep $h = T/N$ low.

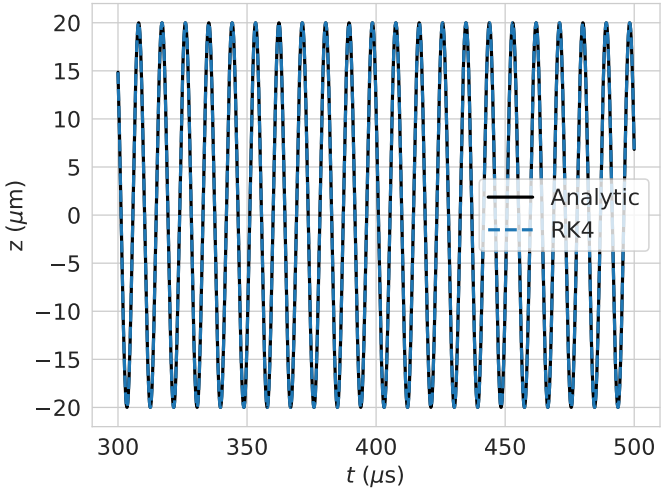

FIG. 6. Vertical motion of a single particle from 300 μs to 500 μs for $N = 5000$. The analytic and RK4 solutions are shown.

Figure 6 shows that the RK4 method agrees with the analytic solution even for a longer time period of 500 μs Based on this we continue using $N = 5000$ time steps and the RK4 method to plot the motion of Particle 1 and Particle 2 in the xy-plane when they do not interact. That is, disregarding the Coulomb force.

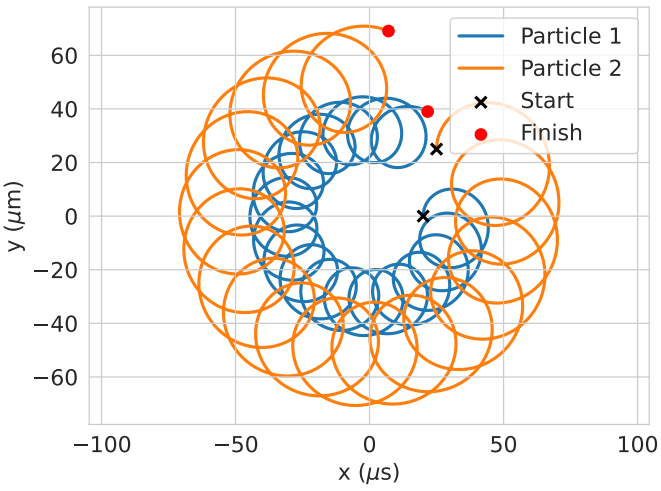

FIG. 7. The horizontal (xy-plane) path of two particles **without interaction** for for $N = 5000$.

In figure 7 The paths have a very similar spiraling shape both resulting circular patterns around the origin.

We continue with the same parameters and particles but now adding the Coloumb force as seen below in figure 8.

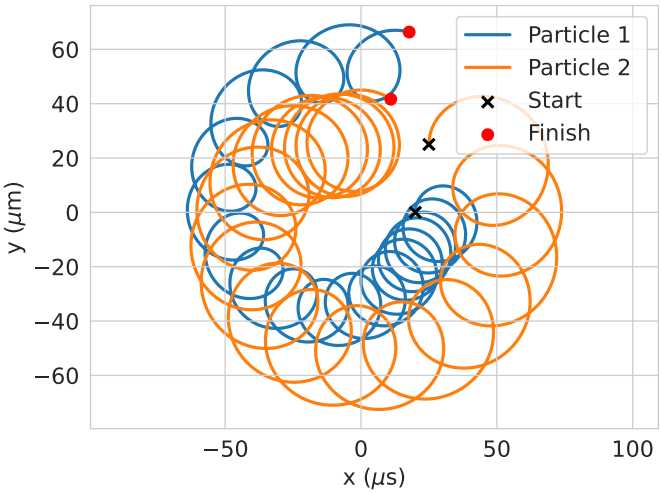

FIG. 8. The horizontal (xy-plane) path of two particles **with interaction** for $N = 5000$.

In figure 8 we see a similar motion as in figure 7. We notice that the paths, although still spiraling, are not as circular as a result of the added Coloumb force.

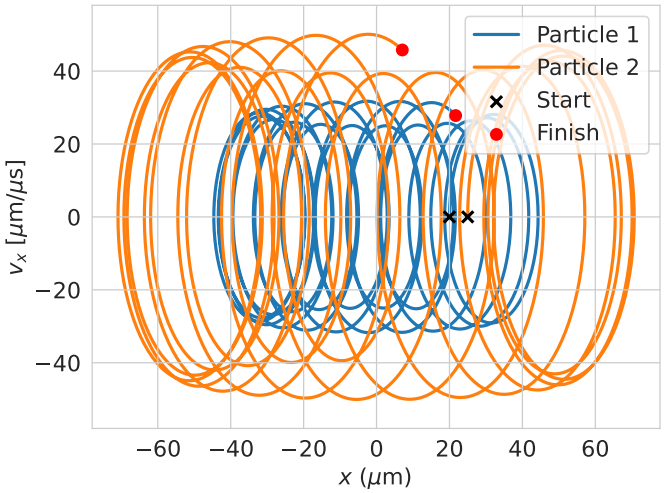

FIG. 9. The phase space (x, v_x) of two particles **without interaction** for $N = 5000$.

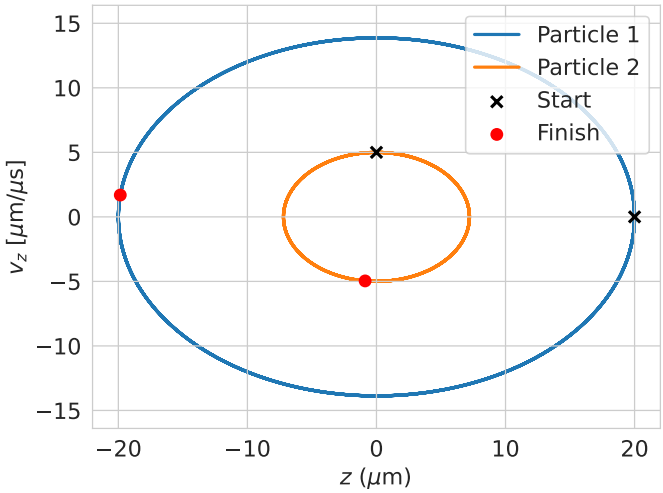

FIG. 11. The phase space (z, v_z) of two particles **without interaction** for $N = 5000$.

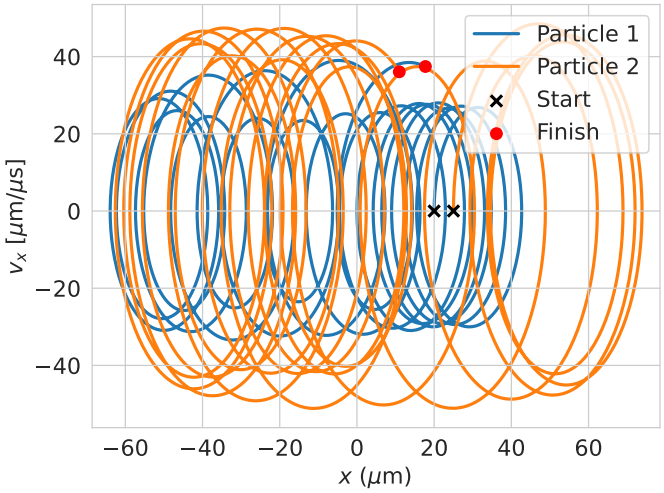

FIG. 10. The phase space (x, v_x) of two particles **with interaction** for $N = 5000$.

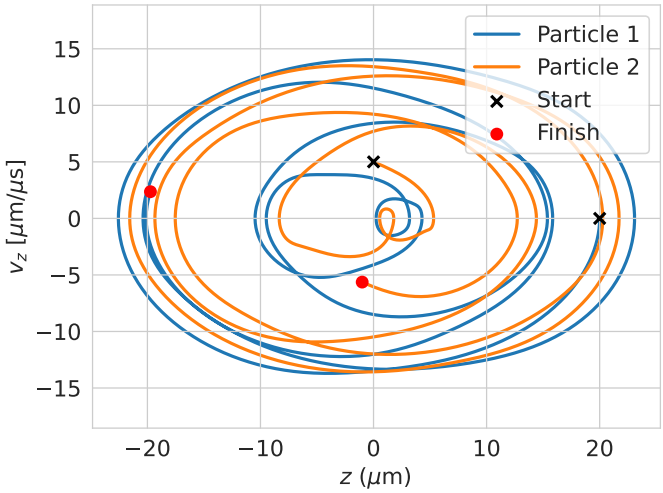

FIG. 12. The phase space (z, v_z) of two particles **with interaction** for $N = 5000$.

The two figures above show the trajectories of Particle 1 and Particle 2 in the (x, v_x) plane. Figure 9 is a simulation disregarding particle interaction whilst figure 10 shows the trajectories with particle interaction. We notice that the trajectories in figure 9 are fairly repetitive whilst figure 10 shows more variations and different final points to figure 9.

Figures 11 and 12 show the trajectories of Particle 1 and Particle 2 in the (z, v_z) plane. In figure 11, without particle interactions, we notice what seems to be repetitive trajectories similarly to figure 9. Figure 12 which includes particle interactions on the other hand displays more irregular trajectories similarly to figure 10.

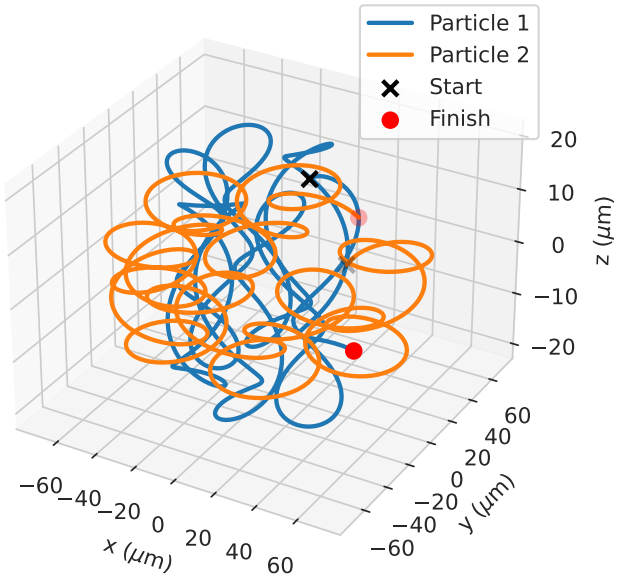

FIG. 13. Shows a 3D representation of two particle paths **without interaction** for $N = 5000$.

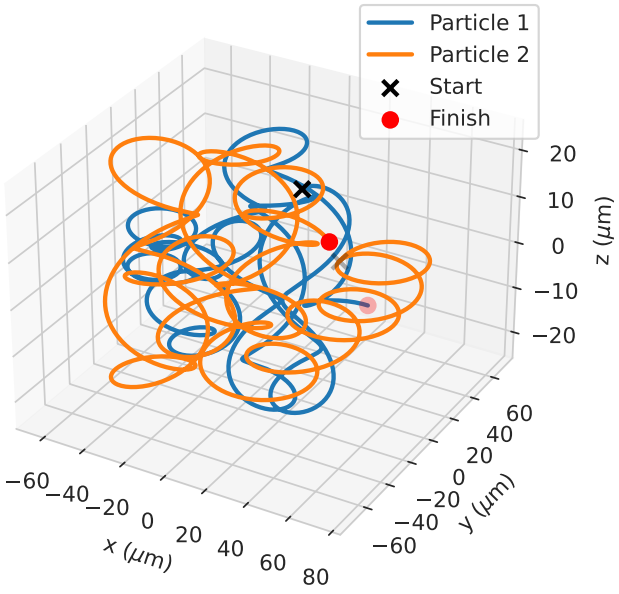

FIG. 14. Shows a 3D representation of two particle paths **with interaction** for $N = 5000$.

Looking at the 3D-plots in figures 13 and 14 it is difficult to follow the exact motion of the particles. Comparing figure 13, without particle interactions, to figure 14, with interactions, one notices that the start positions are identical, yet the finishing positions differ. Taking a close look it is also possible to see differences in the orange and blue lines in the two figures.

Below in figure 15 and 16 we see plots of the relative error of our two numerical methods for different choices of N. We also see the belonging error convergence rate.

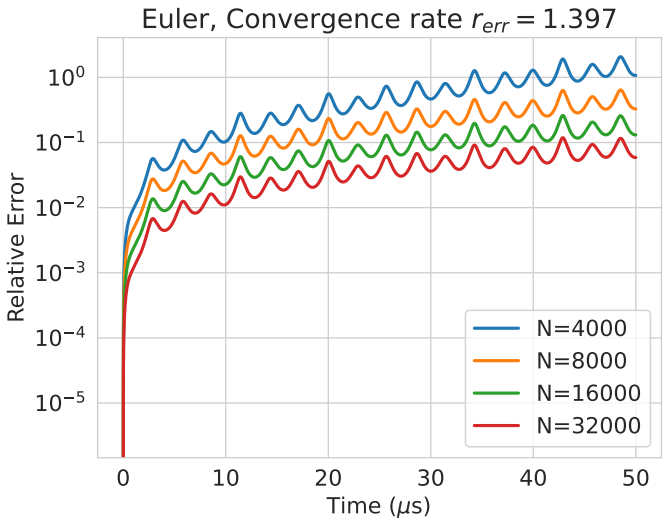

FIG. 15. The plot shows the relative error on a Log scale for a single particle's motion over 50 μs using the forward Euler approximation. The four different lines show results for different step sizes $h = 50/N\mu s$

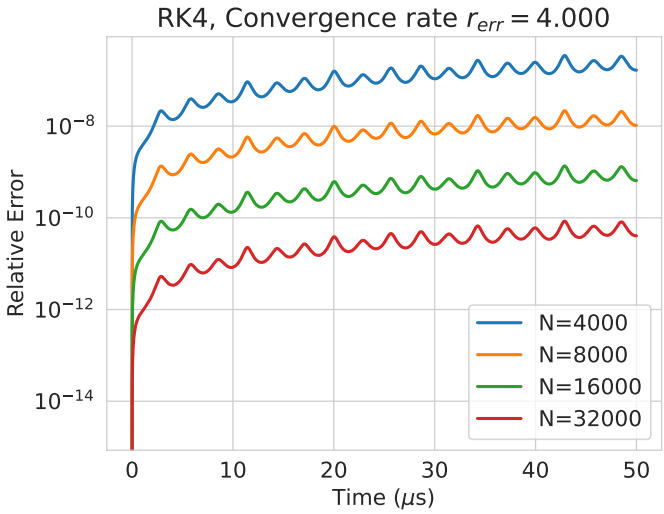

FIG. 16. The plot shows the relative error on a Log scale for a single particle's motion over 50 μs using the fourth order Runge-Kutta approximation. The four different lines show results for different step sizes $h = 50/N\mu s$

Noticeably for both methods, the error decreases as the step size does too (increasing the number of points N) as expected. We see that the error convergence rate of the RK4 method is 4 while the less accurate Euler has a convergence rate of 1.397. Additionally, the logarithmic y-axis of the two figures are of different orders, showing the superiority of the RK4 method giving us more accurate results for $N = 4000$ than Euler manages to do for

$N = 32000$. We also notice an oscillating nature of the relative error over time.

Under in table I, II and III we see the individualy computed error convergence rates for different N and the average as seen in figure 15 and 16.

TABLE I. Error convergence rate for Euler using different values of N where $N_k = 2N_{k-1}$

N_k	8000	16000	32000	**Average**
$r_{\text{err},k}$	1.712	1.325	1.154	**1.397**

TABLE II. Error convergence rate for Euler as in table I using 10 times as big N values

N_k	80000	160000	320000	**Average**
$r_{\text{err},k}$	1.060	1.030	1.015	**1.035**

TABLE III. Error convergence rate for RK4 using different values of N where $N_k = 2N_{k-1}$

N_k	8000	16000	32000	**Average**
$r_{\text{err},k}$	3.999	4.000	4.000	**4.000**

We notice in table III that we for RK4 compute stable error convergence rates for different N. For Euler we see that lower N gives us higher convergence rates, and that even higher N as seen in table II is needed to get convergence rates close to 1.

Under in figure 17 we can see a wide frequency scan for three different amplitudes using a frequency step of 0.02MHz. Here we have again used $N = 5000$ steps for the RK4 method

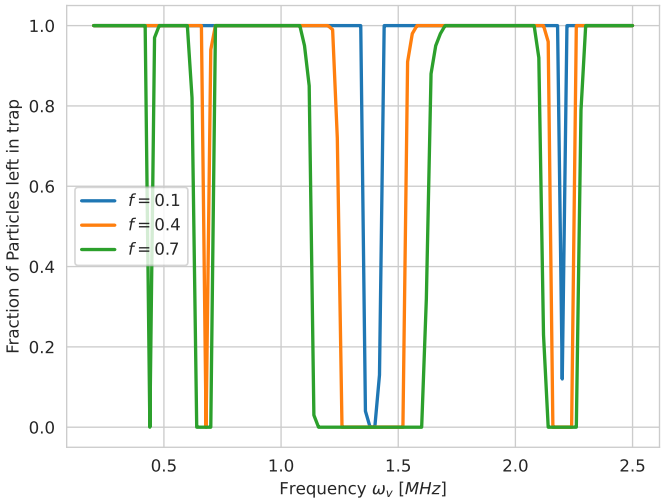

FIG. 17. The plot shows the fraction of particles that are left after 500 μs for angular frequencies $\omega_V \in [0.2, 2.5]$ MHz Each color shows results for a different amplitude f. The simulation is for 100 random particles **without interactions** and $N = 5000$.

We see 4 main frequency bands giving us a resonance in the motion of our particles. These are around a frequency of 0.45, 0.65, 1.4 and 2.2 MHz. We also see that the more narrow resonance bands need a higher amplitude to throw the particles out of the Penningtrap. The most efficient ressonance frequencies are in other words the ones where even an amplitude of 0.1 is enough.

We continue with a frequency analysis and zoom in on frequencies in the interval [2.05, 2.35] MHz for a frequency step of 0.001MHz. This gives us figure 18.

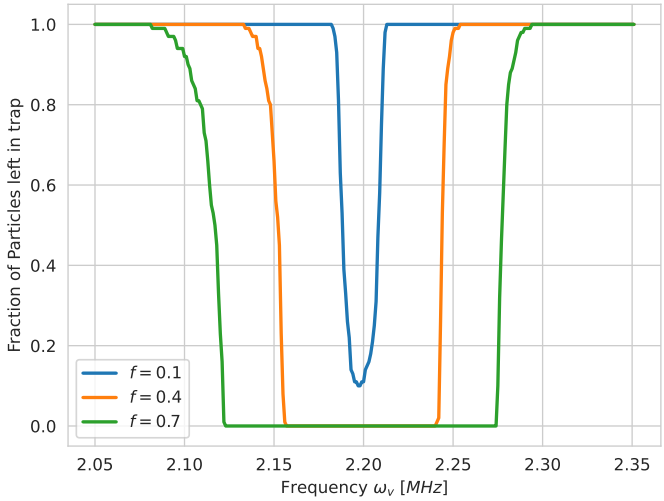

FIG. 18. The fraction of particles that are left after 500 μs for a zoomed in section of the frequency range is shown. The angular frequencies $\omega_V \in [2.05, 2.35]$ MHz are visible. Each color shows results for a different amplitude f. The simulation is for 100 random particles **without interactions** and $N = 5000$.

We see the same as we saw in figure 17 just now with more details giving us a smoother plot.

By turning on particle interaction and looking at the same frequency spectrum we get the following plot in figure 19.

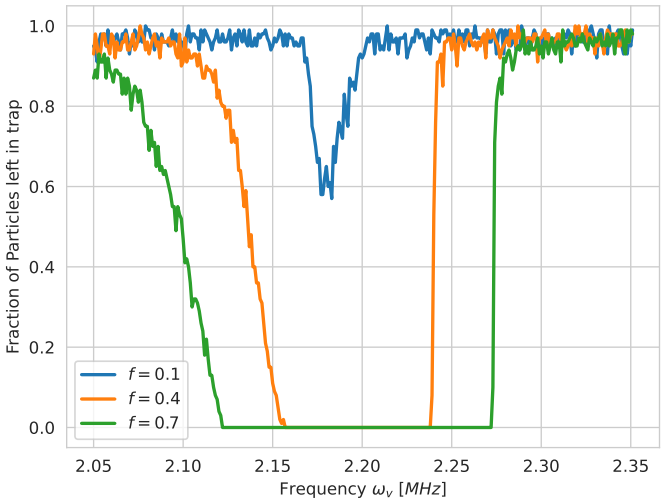

FIG. 19. Shows the fraction of particles that are left after 500 μs for a zoomed in section of the frequency range. The angular frequencies $\omega_V \in [2.05, 2.35]$ MHz are visible. Each color shows results for a different amplitude f. The simulation is for 100 random particles **with interactions** and $N = 5000$.

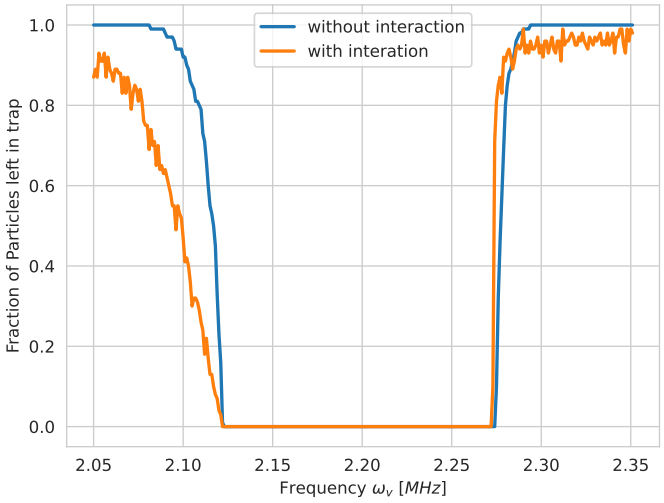

FIG. 20. Comparison of the fraction of particles that are left after 500 μs for $f = 0.7$. The orange line shows results **with interaction** and the blue line results **without interaction**. The angular frequencies $\omega_V \in [2.05, 2.35]$ MHz are visible. The simulation is for 100 particles and $N = 5000$.

We see that some frequencies now resonate more than before and others resonate less. This is especially visible for frequencies from 2.05 to 2.125 for $f = 0.7$ shown in figure 20, which now have lower fractions left in the trap, and for frequencies of around 2.175 for $f = 0.1$ that now have a higher fraction of particles left in the trap. We also see that most frequencies have lost at least some of the particles which compared to figure 17 where mostly all or no particles were lost.

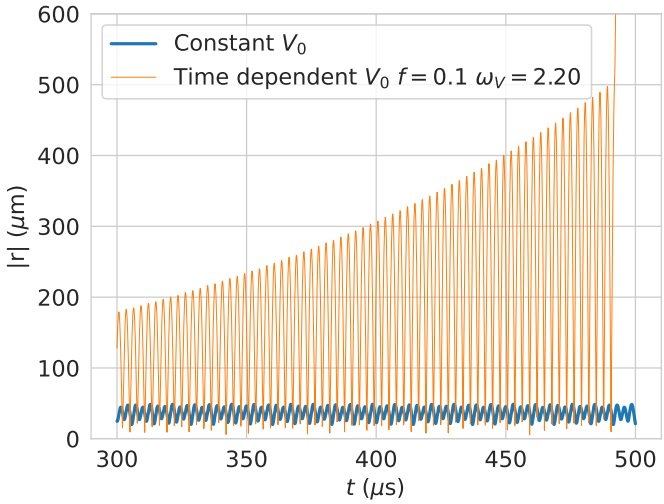

FIG. 21. Here a single particle's (Particle 1) distance from the origin is plotted over time. The blue line represents variations under a constant electromagnetic field V_0. The orange line is for the same particle subjected to a time-dependent electromagnetic field with amplitude $f = 0.1$ and angular frequency $\omega_V = 2.20$. The simulation is run over 500 μs, only 300 to 500 is shown for legibility.

Figure 21 shows a Particle's distance from the center of the Penning trap. One can clearly observe that the particles maximal distance from the origin increases over time when subjected to a time-dependent electromagnetic field until it escapes towards infinity just before 500 μs have passed. When the active electromagnetic field is constant on the other hand, the particles maximal distance does not increase.

IV. DISCUSSION

Initial simulations present results showing the general behavior of our numerical Penning trap. In the comparison of analytic and numerical solutions in figures 2 and 4 the RK4 approximation matches the analytical solution very closely allowing us to use it as the main method for future simulations. The Euler does a reasonable job for the z motion, but gives a poor approximation of the motion in the xy-plane. This is caused by greater directional changes. Seeing the RK4 perform well here and even still for a larger step size in figure 5 allows us to run larger simulations faster since we maintain precision even for a fairly low value of $N = 5000$.

Comparing figure 7 and 8 shows that the Coulomb force has a noticeable effect on the particles motion, this matches expectations from a physical point of view since two positively charged particles will repel each other. This is exactly what happens in figure 8. Here we look at only two particles interacting and the results with and without interactions are not extremely different, but in a case of n particles we would expect larger deviations be-

tween motion with and without interactions for increasing n since all the equations of motion are coupled.

Similarly, there are noticeable differences with and without interactions for the phase space (x, v_x) in figure 9 and 10 and the phase space (z, v_z) in figure 11 and 12. From a physical point of view the results again seem reasonable since the particles repel each other thereby affecting each other's velocities.

The 3D-plots in figure 13, without particle interactions, and figure 14, with interactions allow us to see the full complexity of the particle motion. Already for two particles the paths are hard to follow, and other figures give more valuable information. They do give us a more intuitive representation of particle trajectories in a Penning trap. Especially for the unrealistic case without Coulomb interaction the particles stay within specific boundaries.

In figure 15 and 16 we saw that the RK4 method was more accurate than Euler when comparing to the analytical solution for one particle. This makes sense when it comes to how the two numerical methods work. Euler uses the current position and velocity to step forward which for too large time steps can result in the updated values deviating from the analytical solution. This means that the next forward step will use false values. Calculated values from the Euler method could then go towards infinity even in an atomic scale physics problem. This is avoided using RK4 where the forward stepping is determined by the slope at the beginning, midpoint and end of the interval. This way of stepping forward ensures a stability in our method as well as lowering our global error meaning that we for a too small N only would see inaccurate values but not results going towards infinity. The oscillating behavior of the relative error indicates that our methods perform worse for some particle positions than others. This most likely correlates with the acceleration of the particle as is the case for the Euler method in figure 4. Whilst the particle is on a straight trajectory the approximations will be good, but as it gets redirected towards the center by the magnetic or electric field our numerical methods can't keep up as well.

We also see that the RK4 method has an error convergence rate of 4 which indicates how efficiently the method's error converges towards zero. This value is what we would expect for RK4 based on its global error proportional to the fourth order time step h^4. For Euler on the other hand we would expect a convergence rate of 1. Our value of 1.397 is not exactly 1 which may be a result of the Euler method starting to blow up for $N = 4000$. This would give $\log(\Delta_{\max,k}/\Delta_{\max,k-1})$ a larger negative value which in turn will increase r_{err}. When looking at I this is exactly what we see. The convergence rate calculated for $N_k = 8000$ and $N_{k-1} = 4000$ indicates a global error proportional to h^2. When we look at table II on the other hand we see what we would expect with an error convergence closer to 1, and can therefore conclude that both our methods perform as expected.

Having confirmed an acceptable precision of the RK4 method we move on to larger simulations exploring resonance phenomena. Certain angular frequencies cause all particles to escape whilst others result in all particles remaining as seen in figure 17.

It is clear that a higher amplitude of $f = 0.7$ allows more resonance frequencies, but this does not tell us if these frequencies also resonate for lower amplitudes or not. Here we have not tested to see what happens for a simulation over a longer time period which may be what allows more particles to escape for the lower amplitudes. When we look at figure 21 we see that the increase in length $|\boldsymbol{r}|$ is a slow process that for lower amplitudes would need even more time. At the same time can we from the definition of the magnetic field force $F_B = q\boldsymbol{v} \times \boldsymbol{B}$ see that an amplitude and following velocity increase would influence this restrictive force. This means that a resonating frequency for a lower amplitude may never be enough for some particles to escape. What frequencies and amplitudes gives a stable penning trap is left as possible further research.

Comparing results in figures 18 and 19 we see that particle interaction clearly has an impact on how well the frequencies resonate with the motion of the particles.

The particle interaction seem to allow some particles to escape for almost all frequencies. This can be explained by the randomly generated positions and velocities of our particles. Some of them may be placed so close to each other that the Coloumb force would accelerate them to high enough speeds for them to escape.

We also notice in figure 19 that an amplitude of $f = 0.1$ sees a decrease in the fraction of particles that escape around $\omega_V = 2.2$MHz. This can also be explained by particle interactions. For this amplitude we saw that not every particle escaped in figure 18 which means that this combination of frequencies and amplitude is already not optimal. A slight change of the system by adding particle interactions may be all that was needed to change its balance. This is again only speculations and can not properly be confirmed before a more thorough analysis of the particle trajectories is made. A statistical analysis of the project by performing more computations and taking the average over them would also help us to more accurately explain our results.

V. CONCLUSION

In this section we state three things in a concise manner: what we have done, what we have found, and what should or could be done in the future.

We have investigated the behavior of a Penning trap through numerical simulations, first exploring the basics of the simulation to then focus on resonance phenomena. Our results show that